Temporal variation in relative zircon abundance throughout Earth history

Preprint

C. Brenhin Keller[1,2*], Patrick Boehnke[3,4], and Blair Schoene[5]

[1]Berkeley Geochronology Center, Berkeley, CA 94709
[2]Department of Earth and Planetary Science, University of California, Berkeley, CA 94720
[3]Chicago Center for Cosmochemistry, The University of Chicago, Chicago, IL 60637
[4]Department of the Geophysical Sciences, The University of Chicago, Chicago, IL 60637
[5]Department of Geosciences, Guyot Hall, Princeton University, Princeton, NJ 08544

Abstract

Zircon is the preeminent chronometer of deep time on Earth, informing models of crustal growth and providing our only direct window into the Hadean Eon. However, the quantity of zircon crystallised per unit mass of magma is highly variable, complicating interpretation of the terrestrial zircon record. Here we combine zircon saturation simulations with a dataset of ~52,000 igneous whole-rock geochemical analyses to quantify secular variation in relative zircon abundance throughout Earth history. We find dramatically increasing zircon abundance per mass of magma through geologic time, suggesting that the zircon record underestimates past crustal volume even if preservation bias is eliminated. Similarly, zircons were even less likely to crystallise from low-silica magmas in early Earth history than they are today, together suggesting that the observed Hadean zircon record may require a larger volume of generally felsic Hadean crust than previously expected.

Geochem. Persp. Let. 10.7185/geochemlet.1721

The accessory mineral zircon is ubiquitous, refractory, and readily radiometrically dated to high precision and accuracy through the U and Th decay systems. This trinity of properties has made zircon into a standard mineral tracer of geologic time, resolving timescales from Gyr to kyr through the related U-Th/Pb and U-series geochronometers (*e.g.*, Schoene, 2014; Schmitt, 2011). Zircons constitute the oldest known terrestrial material, providing a glimpse of Earth in the Hadean Eon which has been argued to reveal a remarkably modern environment, complete with liquid water (Mojzsis et al., 2001; Wilde et al., 2001) and felsic crust (Harrison, 2009). Given its ubiquity in igneous rocks, zircon has been used as a proxy for magma crystallisation, crust production, and even crustal composition (Condie et al., 2009; Cawood et al., 2013; Parman, 2015; Lee et al., 2016). However, quantity of zircon is not a direct substitute for quantity of magma or crust. Instead, zircon abundance in the igneous record is a function of magma composition, which is both spatially and temporally heterogeneous. Moreover, due to the high closure temperatures of the U-Th/Pb and U-series systems, ages from these geochronometers exclusively date zircon crystallisation (Schoene, 2014), which need not coincide with the crystallisation of other silicate minerals.

The temperature T_{sat} at which zircon saturates in an igneous magma can be accurately predicted by an empirical equation of the form

$$\frac{a}{T_{sat}} = \ln\left(\frac{[Zr]_{zircon}}{[Zr]_{melt}}\right) + bM + c$$

where a, b, and c are constants, $[Zr]$ is zirconium concentration, and M is a compositional measure of magma polymerisation defined on a molar basis as

$$M = \frac{[Na] + [K] + 2[Ca]}{[Al] * [Si]}$$

(Watson and Harrison, 1983; Boehnke et al., 2013). Purely stochastic heterogeneity in magma composition would produce no meaningful temporal variation in zircon saturation behaviour. However, on sufficiently long geologic timescales, decreasing mantle potential temperature from the early Earth to the present is reflected in systematic variations in average magma composition, including increasing abundance of incompatible elements such as Zr (Keller and Schoene, 2012).

Even within a closed system, magma composition (including M and $[Zr]_{melt}$) varies systematically throughout crystallisation as a function of pressure, temperature, and melt fraction, such that a single bulk zircon saturation temperature is insufficient to characterise the zircon saturation behaviour of simple igneous systems (*e.g.*, Harrison et al., 2007). Accordingly, in order to examine the effects of temporal variations in magma composition throughout Earth history on zircon saturation behaviour, we combine zircon saturation calculations with alphaMELTS (Ghiorso et al., 2002; Smith and Asimow, 2005) major element simulations on 52,300 whole-rock compositions spanning the preserved rock record from modern to Archean. While generally incompatible in silicate minerals, zirconium mineral/melt partition coefficients vary widely between common silicate minerals and may be as high as 0.3-0.5 for clinopyroxene, amphibole, and garnet. Consequently, to ensure accurate zircon saturation calculations, mineral-specific partition coefficients form the Geochemical Earth Reference Model database (GERM, 2013) were used when calculating melt Zr concentrations at each temperature step of each alphaMELTS simulation. Finally, to obtain temporal trends, the results of zircon saturation simulations were subjected to weighted bootstrap resampling following the approach of (Keller and Schoene, 2012) to calculate accurate estimates of the mean and standard error of the mean for each independent variable of interest.

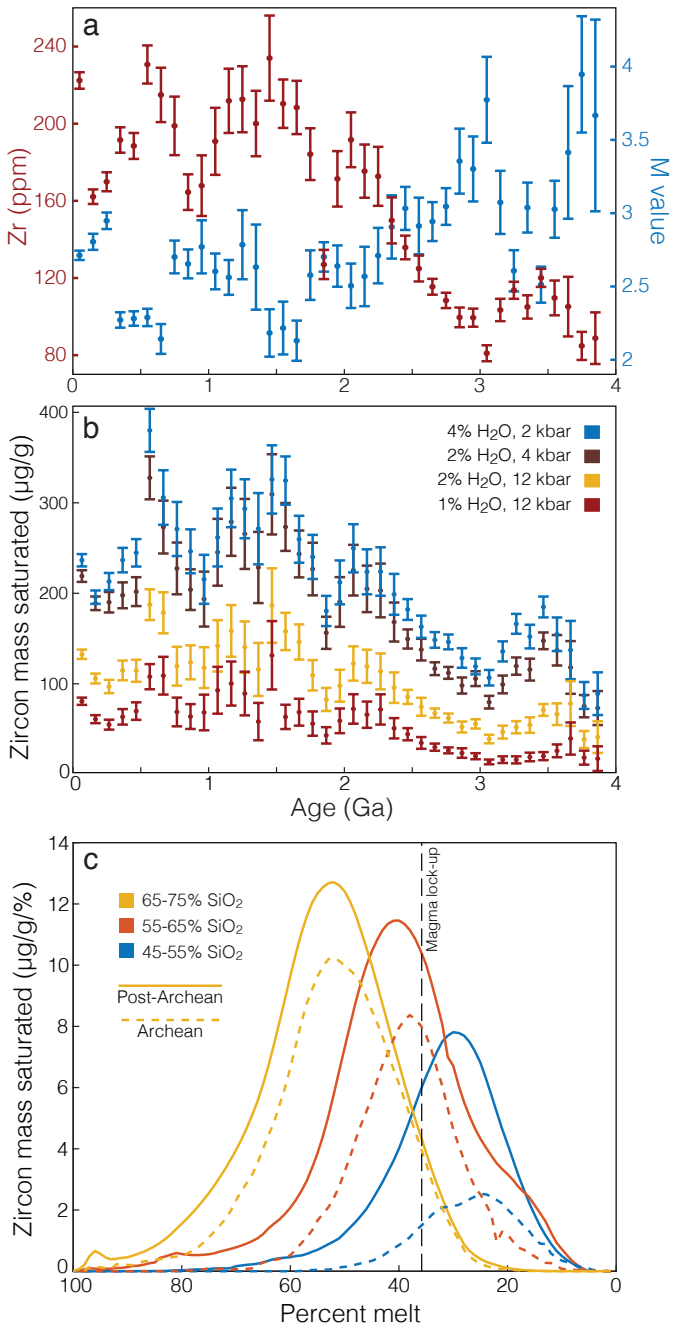

Figure 1: (a) Average zirconium and M value throughout the preserved rock record for continental igneous rocks with 40-80 % SiO_2. (b) Calculated average zircon concentration (micrograms of zircon per gram of whole rock) as a function of time, under a range of possible crystallisation conditions. (c) Zircon saturation distributions during magma crystallisation as a function of percent melt for varying silica ranges, calculated at 6 kilobar and 3 wt. % H_2O. Relative zircon abundance is reported as micrograms of zircon saturated per gram of magma per percentage-point decrease in residual melt fraction. All uncertainties are two-standard-error of the mean.

The primary forcings on zircon abundance over Gyr timescales are illustrated in Figure 1a as averages for igneous whole-rock samples preserved in the present-day continental crust. Over the past 4 Gyr, average igneous zirconium content has increased, while average M-value has decreased. These changes are a consequence of secular mantle cooling, where lower average mantle melting extent has led to increased average concentrations of incompatible elements such as Zr (Keller and Schoene, 2012), and generally lower M values due to lower Ca and higher Al abundance. Combined, these forcings should result in substantially increased zircon concentration in the igneous record (mass of zircon crystallised per mass of magma) since the early Archean.

While zircon saturation is largely independent of magma pressure and water content (Boehnke et al., 2013), the crystallisation of other silicate minerals is not, with higher pressure and lower water content generally increasing crystallisation temperatures. Consequently, in drier or deeper magmas, most silicate minerals will crystallise earlier relative to zircon (Keller et al., 2015); such magmas will be more likely to fully crystallise to the solidus without ever reaching zircon saturation. Correspondingly, saturation simulations run at higher pressures or lower magma water contents display lower total zircon abundance at any given time, as shown in Figure 1b. Nonetheless, common temporal trends are revealed across a wide range of P and H_2O values, with the mass of zircon saturated per mass of magma increasing substantially since the early Archean (Figure 1b). The influence of crystallisation pressure and magma water content on final whole-rock zircon limits our ability to unambiguously reconstruct past magma volumes from the zircon record. However, proposed scenarios of constant or decreasing crustal thickness (*e.g.*, Keller and Schoene, 2012) and constant or increasing magma water content from the Archean to the present would, if anything, accentuate the trends observed in Figure 1.

Changing average zirconium concentration and M value over the past ~4 Gyr have additional consequences for the position of zircon in the magma crystallisation sequence. In general, mafic magmas require greater extents of in-situ differentiation to reach zircon saturation, and thus crystallise zircon at lower residual melt fractions (Figure 1c). As observed in Figure 1c, zircon saturation in Archean magmas of any given silica range is further delayed and diminished due to lower average $[Zr]$ and higher M-values. Unsurprisingly, delayed zircon saturation is directly correlated with lower total zircon mass saturated (Figure 1c), an effect that is accentuated if a magma is not allowed to cool fully to its solidus, either due to eruptive quenching or residual melt extraction.

Due to non-Newtonian magma rheology, magmas containing less than ~37 % melt are disproportionately unlikely to erupt (Caricchi et al., 2007); common volcanic rocks are typically well above this threshold. As residual melt is largely quenched to an amorphous glass upon eruption, any mineral phases crystallising below the eruptive melt fraction will be absent from the volcanic record. Given that basalts display the greatest delay in zircon saturation and are substantially overrepresented in the volcanic record (Keller et al., 2015), the effect of eruptive quenching on zircon saturation will be most noticeable in the mafic record. Phanerozoic basalts typically erupt with fewer

than 30 % phenocrysts by volume (*e.g.*, Bryan, 1983), and at the time of eruption contain little or no zircon, as expected from Figure 1c. Delayed zircon saturation in Archean lithologies should result in an even more pronounced dearth of zircons in the Archean volcanic record for magmas of any given silica content - consistent with the observations of *e.g.*, Kamber et al. (2005) in Eoarchean volcaniclastic metasediments.

As shown in Figure 2a, Archean mafic magmas saturated on average very little zircon per mass of whole-rock both relative to either Archean felsic rocks or post-Archean mafic rocks when crystallised to their solidus at a given set of P, H_2O conditions. This dramatic deficit is equivalent to a difference of more than 10 wt. % silica in whole-rock composition, such that *e.g.*, an Archean granodiorite with 65 wt. % SiO_2 saturates only as much zircon as a Phanerozoic basalt with 53 wt. % SiO_2 (Figure 2b).

Moreover, while felsic magmas in Figure 2a consistently saturate more zircon on average than their mafic counterparts at all times in Earth history, this relative imbalance was stronger in the Archean. Figure 2c illustrates the calculated average mass of zircon saturated during complete crystallisation of a given mass of mafic magma (43-53 % SiO_2) relative to that saturated in an equal mass of coeval felsic magma (63-73 % SiO_2). As observed in Figure 2c, the discrepancy between mafic and felsic zircon abundance is roughly three times greater in the Archean, with Archean mafic magmas crystallising on average little more than a tenth of the zircon mass saturated by an equal mass of coeval felsic magma when both are fully crystallised. This inequality between Archean mafic and felsic zircon abundance is exacerbated when considering magmas that do not fully crystallise, due to the greatly delayed zircon saturation of Archean mafic magmas (Figure 1c) – an effect that would be further compounded by the apparent prevalence of volcanic lithologies in the Archean mafic record (*e.g.*, de Wit and Ashwal, 1997).

If not accounted for, systematic temporal variations in relative zircon abundance would lead to substantial underestimation of the amount of crust required to produce Earth's early zircon record. The impact of this trend on preserved zircon age spectra is shown in Figure 3a, which illustrates how the zircon age spectrum of Voice et al. (2011) would differ if magmas throughout Earth history had crystallised zircon at present-day rates, for a range of assumed model conditions. For magmas crystallising at a given set of P, H_2O conditions, this result is equivalent to the true magma age spectrum required to produce the observed detrital zircon age spectrum in the absence of preservation bias – with true average crystallisation conditions likely intermediate between the shallow/wet and deep/dry endmembers shown in Figure 3a. As peaks in global zircon age spectra are often interpreted as times of increased global magmatic activity, correlated with the plate-tectonic Wilson cycle (Condie and Aster, 2010, *e.g.*,), the corrected age spectrum may imply a more steady-state supercontinent cycle with similar maxima in magmatic activity to ~3 Ga, or (depending on the strength of preservation bias) even before.

The zircon abundance correction increases the magmatic significance of the Archean and Proterozoic zircon record, and appears to improve the correspondence in magnitude between temporally correlated zircon abundance maxima and mantle depletion events (*e.g.*, Pearson et al., 2007). Considering present-

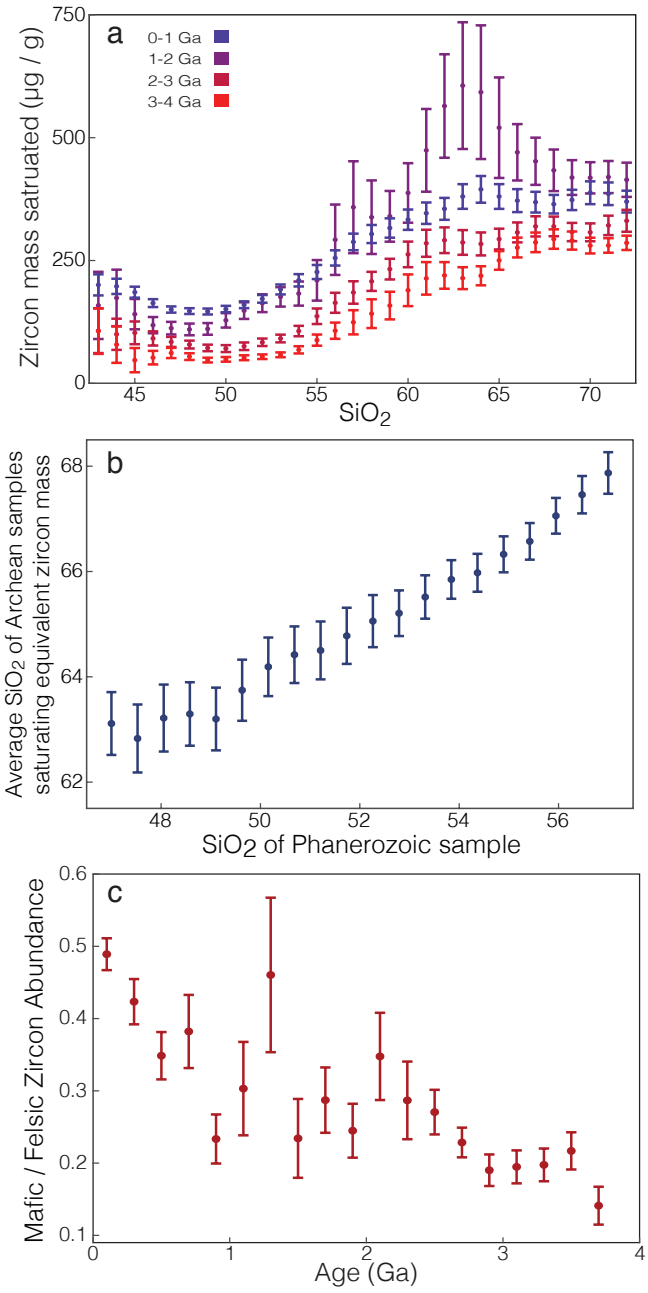

Figure 2: Temporal variability in the distribution of zircon between igneous rocks of different silica contents, calculated at 6 kilobar and 3 wt. % H_2O. (a) Temporal variation in relative zircon abundance as a function of silica. (b) Line of silica equivalence between Archean and Phanerozoic samples (the silica contents required to saturate the same mass of zircon in Archean and Phanerozoic magmas). (c) The mass of zircon saturated per mass of mafic magma (43-53 % SiO_2) relative to that saturated in an equivalent mass of coeval felsic magma (63-73 % SiO_2). The likelihood of saturating zircon in mafic lithologies was dramatically lower (by nearly factor of 5) in the earliest Archean than it was today. All uncertainties are two-standard-error of the mean.

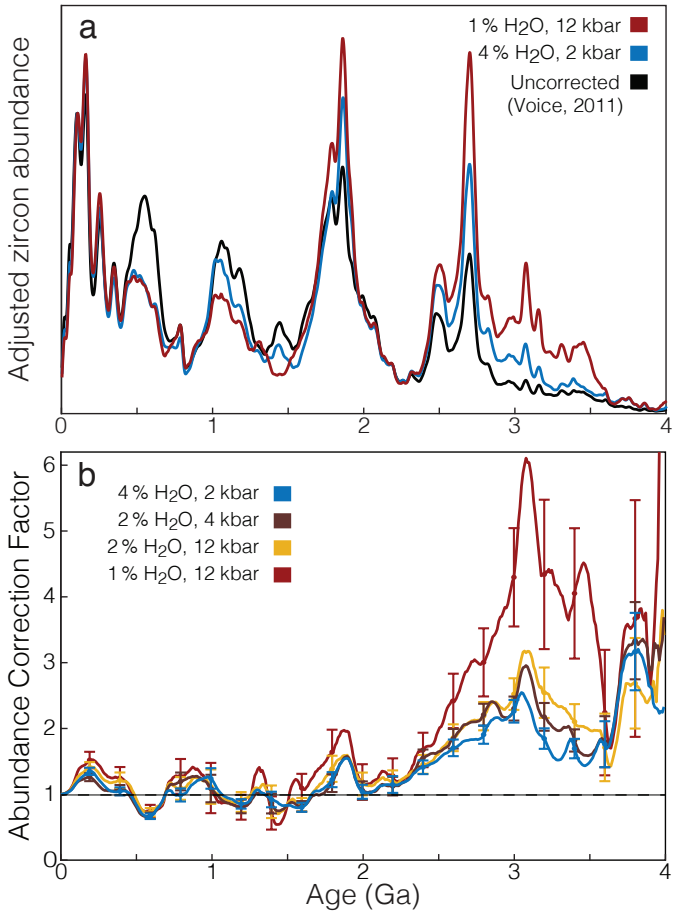

Figure 3: (a) The effect of applying a relative zircon abundance correction (normalising to constant magma zircon productivity) to the detrital zircon age spectrum of Voice et al. (2011) for varying crystallisation conditions. (b) The average mass of magma throughout Earth history required to produce the same mass of zircon as a unit mass of average present-day magma.

day zircon productivity levels, three to five times more Archean magma was required to produce a given amount of zircon (Figure 3b); such corrections should be applied to models relying on zircon abundance as a proxy for crust or magma extent.

If Hadean mantle potential temperatures were equal to or greater than those of the early Archean, we might infer that zircon saturation was inhibited in Hadean mafic magmas by a factor equal to or greater than that of the early Archean. This would decrease the likelihood that any given Hadean zircon originated from a mafic lithology by more than a factor of three relative to an equivalent model where systematic temporal trends in whole-rock geochemistry are neglected.

While the above considerations are applicable in principle to zircon-based crustal growth models such as those of Belousova et al. (2010) or Dhuime et al. (2012), a simple correction factor as in Figure 3b alone is likely insufficient. Firstly, applying the models of Figure 3 to a crustal growth curve assumes closed-system crystallisation at crustal scale. While this may seem a minor assumption, it does not necessarily hold in the early Hadean: a terrestrial flotation cumulate, for instance, would systematically exclude dense zircon. Consistent with this expectation, lunar anorthosites contain only 0.1-0.5 ppm zirconium (*e.g.*, several hundred times lower than an average Archean basalt), offset by zirconium enrichments up to 2000 ppm in complimentary KREEP basalts (Ehmann et al., 1979). Such extreme zirconium deficiency in Lunar anorthosites indicates that the most likely candidate lithology for primordial terrestrial crust is effectively invisible to zircon-based crustal growth models. Secondly, the insensitivity of zircon saturation to water content along with Zr immobility in aqueous fluid implies that most subducted zircon will not return to the crust in new arc magmas – a corollary to the well-known arc signature of high-field-strength element depletion. Consequently, while zircon-based crustal growth models account for crustal magmatic reworking, crustal destruction by sediment subduction and subduction-erosion will be largely undetectable in the zircon record. Together, these specific issues arising from the crystallisation and stability of zircon suggest that both initial crustal volume and subsequent net growth or destruction rate are poorly bounded and subject to assumptions (*e.g.*, Supplementary Figure 4).

Together, our results emphasise the significance of the extant zircon record of early Earth history, given the difficulty of saturating zircon under early Earth conditions due to lower average magma zirconium content and lower silicate magma polymerisation state. Under such conditions, zircon saturation is delayed and diminished, especially in mafic lithologies. Consequently, more crust is required to explain preserved zircon age spectra, and a potentially significant volume of felsic crust is favoured as the likely source of preserved Hadean zircons.

METHODS

Zircon saturation

In order to quantify the effects of changing magma composition on zircon abundance throughout Earth history, we calculated the expected mass of zircon saturated per unit mass of rock for 52,300 igneous whole-rock compositions with defined major-element and Zr contents from the dataset of Keller and Schoene (2012), integrating alphaMELTS equilibrium crystallisation simulations with zirconium partitioning calculations and the zircon saturation thermometer of Boehnke et al. (2013). For each whole-rock composition, a pMELTS-mode alphaMELTS (Ghiorso et al., 2002; Asimow et al., 2004; Smith and Asimow, 2005) isobaric batch equilibrium crystallisation simulation was run from the liquidus to the solidus in 10 C increments, recording the composition of the melt and all mineral phase proportions at each crystallisation step. At each step, the zircon saturation state was assessed by calculating the concentration of zirconium in the melt in the absence of zircon using the reported mineral phase proportions along with GERM mineral/melt Zr partition coefficients for each phase present, and comparing that to the concentration of zirconium required to saturate zircon at that temperature and major element composition using the equations of Boehnke et al. (2013). From these concentrations along with the remaining melt fraction, we calculate the total mass of extant zircon (if any) at each temperature step, as well as the differential zircon growth (if any) for each cooling increment. As discussed in the text, full simulations for each whole-rock sample were conducted at a range of P, H_2O conditions in order to quantify the effect of crystallisation pressure and water content on total mass of zircon saturated. While all simulations were run with an initial oxygen fugacity one log unit above the fayalite-magnetite-quartz redox

buffer, compared to changes in crystallisation pressure or magma water content, magma redox state has negligible effect on melt zirconium content during equilibrium crystallisation.

Following these simulations, a resultant dataset recording the total mass of zircon saturated by the end of crystallisation for each whole-rock sample at a given set of P, H_2O conditions was then subjected to the weighted bootstrap resampling procedure of Keller and Schoene (2012) (with location, age, and age uncertainty as reported for each sample in the dataset) in order to evaluate the variation in average zircon abundance throughout the preserved rock record (*e.g.*, Figure 1). Finally, an intermediate set of P, H_2O conditions (6 kbar, 3 wt. % H_2O) were chosen to illustrate in more detail the typical consequences of lower Archean zirconium content, including delayed and diminished zircon saturation throughout the crystallisation process (Figure 1c) and particularly diminished zircon saturation in mafic lithologies (Figure 2).

Qualitatively, the effect of in-situ magmatic differentiation is to drive up zirconium concentration in the residual melt, while at the same time reducing the minimum zirconium concentration required to saturate zircon due to declining temperature and M (Supplementary Figure 1). Zircon saturation occurs when the two trends intersect, resulting in earlier saturation and higher saturation temperatures than in a bulk crystallisation model where melt evolution is ignored. Consequently, as seen in Supplementary Figure 2, corrected saturation temperatures universally exceed bulk saturation temperatures, particularly for samples which successfully saturate zircon. Similarly, corrected zircon saturation temperatures also necessarily exceed average zircon crystallisation temperatures for the same sample, though to a lesser degree.

While slightly counterintuitive, the effect of high crystallization pressure or low magma water content to decrease the total mass of zircon saturated is ultimately related to zirconium partitioning in silicate mineral phases other than zircon. Decreasing water content or increasing crystallization pressure increases the temperature at which most silicate minerals begin to crystallise, but has little or no effect on zircon saturation temperature, thus moving silicate crystallization forward relative to zircon saturation, or (equivalently) delaying zircon saturation as a function of percent crystallinity. While zirconium is generally incompatible in major rock-forming minerals, it is only slightly incompatible (or even approaches compatibility) in a range of important major and minor rock-forming minerals, and increases in compatibility as a function of melt SiO_2 (Supplementary Figure 3) with the net result that bulk solid/melt Zr partition coefficients for relevant mineral assemblages are typically greater than 0.05 and may exceed 0.2. Consequently, delaying zircon saturation may dramatically limit the amount of Zr available to form zircon, particularly in the case of gradual closed-system crystallization that approaches equilibrium partitioning. For example, if zircon saturation can be delayed until a bulk magma has reached 1 % melt remaining, even with a Kd of 0.1 (ten times greater zirconium concentration in the melt), the solid still contains roughly ten times more total zirconium than the remaining melt due to the 99-fold advantage of the solid in the total mass balance, and at most only 1/10th of the total zirconium is available at this point to crystallize zircon. This effects is illustrated in Supplementary Figure 3b for a range of potential bulk solid/melt partition coefficients. This effect is compounded in the event that the residual melt from bulk crystallization of a given magma tends towards peralkaline compositions (as is not uncommon) due to the high zircon solubility of peralkaline magmas, which is sufficiently extreme that, for a range of expected crystallization paths, "once zircon becomes unstable due to [an] increase in peralkalinity, the melt can never regain zircon saturation by continued feldspar crystallization" Watson (1979). As a result, delaying zircon saturation tends to markedly reduce the total mass of zircon saturation even in the absence of eruptive quenching.

Applications to magma volume and crustal growth

A zircon abundance correction factor as a function of crystallisation age (*i.e.* a scaling from zircon abundance to magma or crust volume) as in Figure 3b may be calculated by taking the inverse of the zircon abundance curve (Figure 1b) and standardizing to a value of 1 at the present. This correction may in principle be extended to zircon Hf model ages based on the crystallisation age of zircons with a given model age, and thence to crustal growth models. However, as discussed in the text, a single correction factor is likely insufficient to fully correct a zircon-based integrated crustal growth curve due to uncertainties regarding initial crustal volume and crustal return flux to the mantle via processes and lithologies that (for reasons of zircon stability and crystallization systematics) do not leave a clear record in the crustal zircon archive.

To show the paractical impact of such uncertainties, Supplementary Figure 4 illustrates how the crustal growth curve of Dhuime et al. (2012) might be altered in a range of plausible scenarios. In particular, the initial volume of primary crust circa 4.5 Ga is poorly bounded, considering the possibility for a nearly zirconium-free primary crust, analogous to the anorthosite flotation cumulate of the lunar highlands. The Lunar anorthosite highlands are 60-100 km thick and cover a majority of the lunar surface (presumably all, at formation), with the net result that the lunar crust comprises 12 % of the volume of the moon Taylor (1989). The maximum thickness of an equivalent terrestrial floatation crust would be limited by the maximum pressure of feldspar stability considering terrestrial gravity, but even a comparatively modest ~20 km thick global flotation crust would represent roughly twice the modern volume of continental crust. Absent an assumption of zero initial cumulate crust, the slope of the crustal volume curve is be poorly constrained by the zircon record. There is no requirement from zircon geochemistry or age spectra that the mass flux from the mantle to the crust should exceed that from the crust to the mantle, and thus no requirement that net crustal growth rate should be positive. While intracrustal reworking may be estimated from the continental zircon record (*e.g.*, Belousova et al., 2010; Dhuime et al., 2012), crustal destruction by recycling to the mantle is not similarly constrained, and this mantle recycling term need not be small. Isotopic estimates suggest that crustal recycling to the mantle should consume roughly 0.35 crustal volumes per Gyr, or the entire present-day crustal volume in less that 3 Gyr (DePaolo, 1983). Supplementary Figure 4 illustrates several potential scenarios ranging from zero to twenty kilometers of primary crust and various functional forms for the recycling rate. However, all illustrated recycling rates are monotonic, which need not be the case; instead, it is entirely possible that maxima in crustal destruction match those in crustal production (*e.g.*, Figure 3a), such that episodic peaks in crust production may or may not result in episodes of net crustal growth. We conclude that both the initial boundary condition and subsequent evolution of the crustal volume curve may vary widely, leading to substantial uncertainty in crustal volume curves.

AUTHOR CONTRIBUTIONS

C.B.K. conducted the calculations and prepared the manuscript. All authors contributed to the design of the study and the interpretation of the results.

ACKNOWLEDGEMENTS

C.B.K. was supported by the Department of Energy Computational Science Graduate Fellowship Program of the Office of Science and National Nuclear Security Administration in the Department of Energy under contract DE-FG02-97ER25308. Computational resources were provided by the Princeton Institute for Computational Science and Engineering.

DATA AVAILABILITY

All data and source code used in this study is freely available at https://github.com/brenhinkeller/meltstzirc.

REFERENCES

Asimow, P.D., Dixon, J.E., and Langmuir, C.H., 2004, A hydrous melting and fractionation model for midocean ridge basalts: Application to the MidAtlantic Ridge near the Azores: Geochemistry Geophysics Geosystems, v. 5.

Belousova, E., Kostitsyn, Y., Griffin, W.L., Begg, G.C., O'Reilly, S.Y., and Pearson, N.J., 2010, The growth of the continental crust: Constraints from zircon Hf-isotope data: LITHOS, v. 119, p. 457–466.

Boehnke, P., Watson, E.B., Trail, D., Harrison, T.M., and Schmitt, A.K., 2013, Zircon saturation re-revisited: Chemical Geology, v. 351, p. 324–334.

Bryan, W.B., 1983, Systematics of modal phenocryst assemblages in submarine basalts: Petrologic implications: Contributions to Mineralogy and Petrology, v. 83, p. 62–74.

Caricchi, L., Burlini, L., Ulmer, P., and Gerya, T., 2007, Non-Newtonian rheology of crystal-bearing magmas and implications for magma ascent dynamics: Earth and Planetary Science Letters, v. 264, p. 402–419.

Cawood, P.A., Hawkesworth, C.J., and Dhuime, B., 2013, The continental record and the generation of continental crust: Geological Society of America Bulletin, v. 125, p. 14–32.

Condie, K.C. and Aster, R.C., 2010, Episodic zircon age spectra of orogenic granitoids: The supercontinent connection and continental growth: Precambrian Research, v. 180, p. 227–236.

Condie, K.C., Belousova, E., Griffin, W.L., and Sircombe, K.N., 2009, Granitoid events in space and time: Constraints from igneous and detrital zircon age spectra: Gondwana Research, v. 15, p. 228–242.

de Wit, M.J. and Ashwal, L.D., 1997, Greenstone belts: Oxford University Press.

DePaolo, D.J., 1983, The mean life of continents: Estimates of continent recycling rates from Nd and Hf isotopic data and implications for mantle structure: Geophysical Research Letters, v. 10, p. 705–708.

Dhuime, B., Hawkesworth, C.J., Cawood, P.A., and Storey, C.D., 2012, A Change in the Geodynamics of Continental Growth 3 Billion Years Ago: Science, v. 335, p. 1334–1336.

Ehmann, W.D., Chyi, L.L., Garg, A.N., and Ali, M.Z., 1979, The distribution of zirconium and hafnium in terrestrial rocks, meteorites and the moon : Physics and Chemistry of the Earth, v. 11, p. 247–259.

GERM, 2013, Geochemical Earth Reference Model Partition Coefficient Database: .

Ghiorso, M.S., Hirschmann, M.M., Reiners, P.W., and Kress, III, V.C., 2002, The pMELTS: A revision of MELTS for improved calculation of phase relations and major element partitioning related to partial melting of the mantle to 3 GPa: Geochemistry Geophysics Geosystems, v. 3, p. 1–36.

Harrison, T.M., 2009, The Hadean Crust: Evidence from >4 Ga Zircons: Annual Review of Earth and Planetary Sciences, v. 37, p. 479–505.

Harrison, T.M., Watson, E.B., and Aikman, A.B., 2007, Temperature spectra of zircon crystallization in plutonic rocks: Geology, v. 35, p. 635.

Kamber, B.S., WHITEHOUSE, M., BOLHAR, R., and Moorbath, S., 2005, Volcanic resurfacing and the early terrestrial crust: Zircon U–Pb and REE constraints from the Isua Greenstone Belt, southern West Greenland: Earth and Planetary Science Letters, v. 240, p. 276–290.

Keller, C.B. and Schoene, B., 2012, Statistical geochemistry reveals disruption in secular lithospheric evolution about 2.5Gyr ago: Nature, v. 485, p. 490–493.

Keller, C.B., Schoene, B., Barboni, M., Samperton, K.M., and Husson, J.M., 2015, Volcanic–plutonic parity and the differentiation of the continental crust: Nature, v. 523, p. 301–307.

Lee, C.T.A., Yeung, L.Y., McKenzie, N.R., Yokoyama, Y., Ozaki, K., and Lenardic, A., 2016, Two-step rise of atmospheric oxygen linked to the growth of continents: Nature Geoscience, v. 9, p. 417–424.

Mojzsis, S.J., Harrison, T.M., and Pidgeon, R.T., 2001, Oxygen-isotope evidence from ancient zircons for liquid water at the Earth's surface 4,300 Myr ago: Nature, v. 409, p. 178–181.

Parman, S.W., 2015, Time-lapse zirconography: Imaging punctuated continental evolution: Geochemical Perspectives Letters, v. 1, p. 43–52.

Pearson, D.G., Parman, S.W., and Nowell, G.M., 2007, A link between large mantle melting events and continent growth seen in osmium isotopes : Nature, v. 449, p. 202–205.

Schmitt, A.K., 2011, Uranium Series Accessory Crystal Dating of Magmatic Processes: Annual Review of Earth and Planetary Sciences, v. 39, p. 321–349.

Schoene, B., 2014, 4.10 U–Th–Pb Geochronology: In R.L. Rudnick (ed.), *Treatise on Geochemistry*, p. 341–378, Elsevier.

Smith, P.M. and Asimow, P.D., 2005, Adiabat 1ph: A new public front-end to the MELTS, pMELTS, and pHMELTS models: Geochemistry Geophysics Geosystems, v. 6, p. 1–8.

Taylor, S.R., 1989, Growth of planetary crusts: Tectonophysics, v. 161, p. 147–156.

Voice, P.J., Kowalewski, M., and Eriksson, K.A., 2011, Quantifying the Timing and Rate of Crustal Evolution: Global Compilation of Radiometrically Dated Detrital Zircon Grains: The Journal of Geology, v. 119, p. 109–126.

Watson, E.B., 1979, Zircon saturation in felsic liquids: Experimental results and applications to trace element geochemistry: Contributions to Mineralogy and Petrology, v. 70, p. 407–419.

Watson, E.B. and Harrison, T.M., 1983, Zircon saturation revisited: temperature and composition effects in a variety of crustal magma types: Earth and Planetary Science Letters, v. 64, p. 295–304.

Wilde, S.A., Valley, J.W., Peck, W.H., and Graham, C.M., 2001, Evidence from detrital zircons for the existence of continental crust and oceans on the Earth 4.4 Gyr ago: Nature, v. 409, p. 175–178.

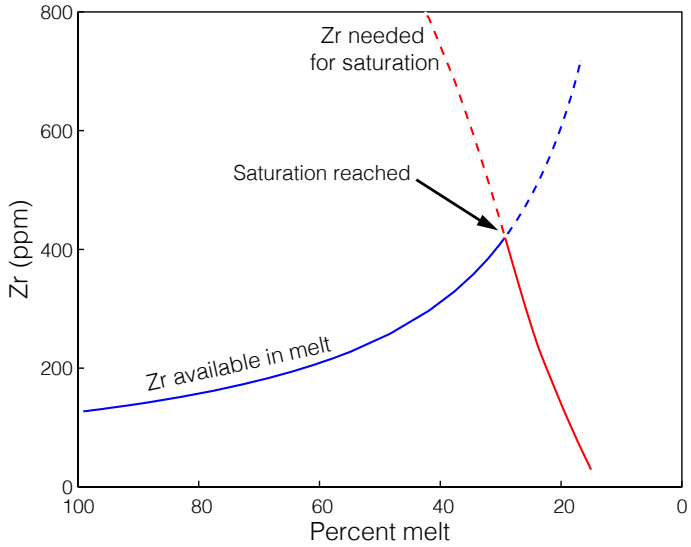

Supplementary Figure 1: Zirconium evolution and the point of zircon saturation during a crystallization simulation for a single whole-rock composition, in this case a basaltic andesite composition. Zirconium concentration in the melt increases during differentiation as a generally incompatible element, while both temperature and M-value decrease with increasing crystallinity, decreasing the zirconium concentration required to saturate zircon.

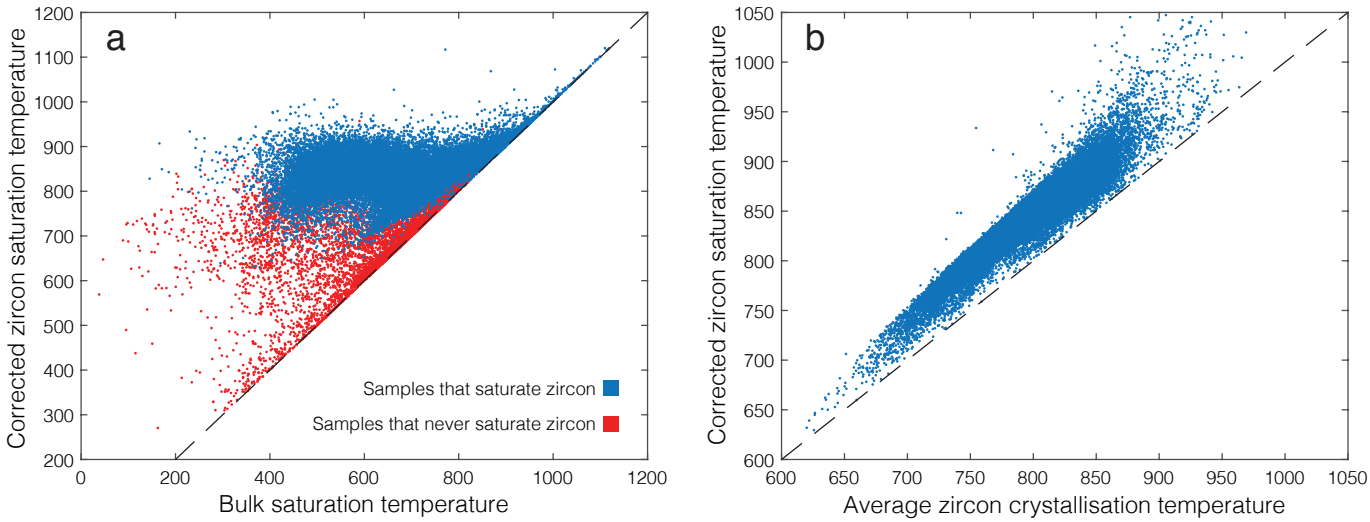

Supplementary Figure 2: The relationship between bulk zircon saturation temperatures, corrected zircon saturation temperatures, and average zircon crystallisation temperatures during closed-system equilibrium crystallisation for 52,300 whole-rock compositions. Bulk saturation temperature is the result of applying the equation of Boehnke et al. (2013) directly to each whole-rock composition. (a) Corrected zircon saturation temperature adjusts for differentiation during in-situ crystallisation, resulting in consistently higher saturation temperatures relative to bulk saturation temperature, as observed in panel. For samples that do not ever saturate zircon, the highest saturation temperature of any differentiated melt is reported. (b) For samples which do saturate zircon, average zircon crystallisation temperature is the weighted average of the zircon crystallisation temperature distribution, resulting in temperatures closely correlated with but necessarily colder than the adjusted zircon saturation temperature. While not highly sensitive to pressure or water content, the values shown here are calculated for shallow, water saturated conditions (2 kbar and 4wt % H_2O).

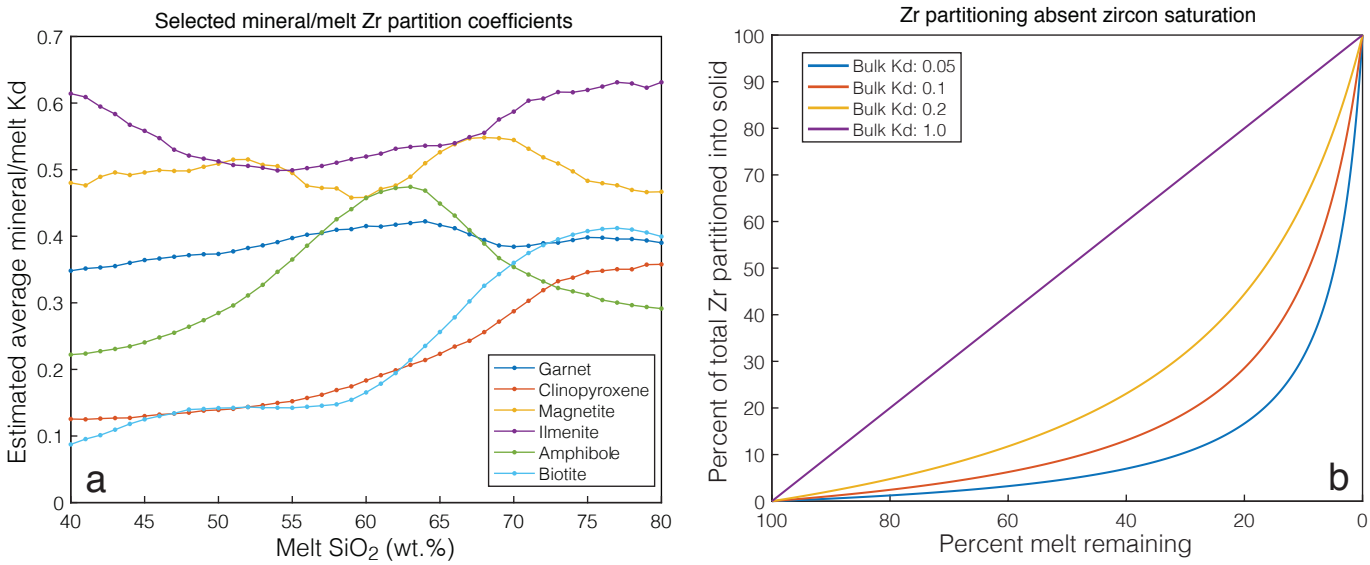

Supplementary Figure 3: Zirconium partitioning. (a) Zirconium mineral/melt partition coefficients for several minerals with non-negligible zirconium compatibility. Partition coefficients shown are averages of GERM partition coefficient data fit as a function of melt SiO_2. Uncertainties are omitted for visibility. (b) The proportion of the total zirconium budget partitioned into the solid at equilibrium as a function of remaining melt percent and mineral/melt partition coefficient.

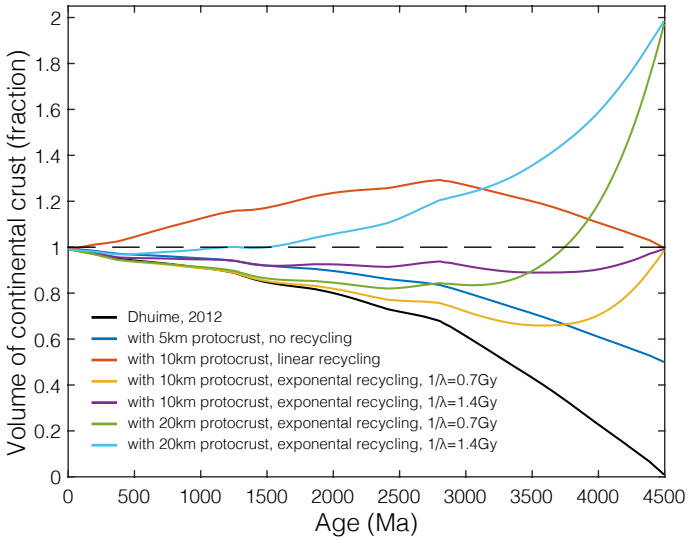

Supplementary Figure 4: A selection of possible crustal growth curves with varying initial boundary conditions (no crust, 5, 10, and 20km thick primordial anorthosite floatation crust) and functional form of the recycling term (none, linear, and exponential with 0.7 or 1.4 Ga e-folding time $1/\lambda$). Exponential recycling rates are considered based on the possibility that crustal recycling rate may have been faster in the past as a direct and indirect result of higher mantle potential temperature.